Journal of Biomolecular NMR, 5 (1995) 95–105
ESCOM

J-Bio NMR 262

Determination of heteronuclear three-bond J-coupling constants in peptides by a simple heteronuclear relayed E.COSY experiment

Jürgen M. Schmidt[a,*], Richard R. Ernst[a,**], Saburo Aimoto[b] and Masatsune Kainosho[c]

[a]*Laboratorium für Physikalische Chemie, Eidgenössische Technische Hochschule, Universitätsstrasse 22, CH-8092 Zürich, Switzerland*
[b]*Institute for Protein Research, Osaka University, Osaka 565, Japan*
[c]*Department of Chemistry, Tokio Metropolitan University, Hachioji 192-03, Japan*

Received 26 July 1994
Accepted 2 January 1995

Keywords: 2D heteronuclear NMR; Isotope labeling; Coupling constants; Antamanide

Summary

A simple heteronuclear relayed E.COSY pulse sequence with a minimum number of pulses is proposed for the quantitative determination of heteronuclear three-bond J-coupling constants in uniformly ^{13}C-enriched polypeptide samples. Numerous heteronuclear three-bond coupling constants, including $^3J_{H^NC'}$, $^3J_{H^NC\beta}$, $^3J_{H\beta C'}$, and $^3J_{H\alpha C\gamma}$, can be determined for each residue from a single heteronuclear relayed E.COSY spectrum. Couplings relevant for stereospecific assignments as well as for the determination of dihedral angles in the amino acid backbone and in side chains are obtained. The method is demonstrated on the uniformly ^{13}C-enriched decapeptide antamanide (-Val[1]-Pro[2]-Pro[3]-Ala[4]-Phe[5]-Phe[6]-Pro[7]-Pro[8]-Phe[9]-Phe[10]-).

Introduction

The determination of the three-dimensional structure of peptides and proteins in solution by NMR relies on distance constraints derived from cross-relaxation measurements (Wüthrich, 1986). In recent years, more and more investigations have also taken advantage of angular constraints obtained from the measurement of vicinal J-coupling constants, applying Karplus relations (Karplus, 1959,1963). Based on a single vicinal J-coupling constant, it is impossible to uniquely determine a dihedral angle, due to a multivalued relation. The ambiguity can be removed by measuring several coupling constants that depend differently on the same dihedral angle. This requires, in addition to the measurement of the traditionally preferred homonuclear $^1H,^1H$ coupling constants, also the determination of heteronuclear coupling constants which also fulfill Karplus-relation-like dependencies on the dihedral bond angle (Wasylishen and Schaefer, 1972; Bystrov, 1976; Fishman et al., 1979).

Although procedures have been reported for the accurate measurement of heteronuclear coupling constants involving rare nuclei in natural abundance (Schmieder et al., 1991), for larger biopolymers it is of great advantage to have ^{13}C- and/or ^{15}N-labelled molecules available. Numerous techniques have been described in the literature, taking advantage of isotopically enriched proteins, to determine ^1H-^{13}C, ^1H-^{15}N, ^{15}N-^{13}C and ^{13}C-^{13}C coupling constants. The most simple approach for the measurement of ^1H-^{13}C and ^1H-^{15}N couplings exploits the heteronuclear J-splittings apparent in conventional homonuclear proton two-dimensional spectra (Montelione et al., 1989; Montelione and Wagner, 1989; Wider et al., 1989; Edison et al., 1991). In fact, heteronuclear coupling constants can be read off directly from the cross-peak multiplet structures in homonuclear two-dimensional spectra. Large heteronuclear one-bond couplings are employed for separating two 2D multiplet patterns along one dimension (usually ω_1) in an E.COSY (exclusive correlation spectroscopy) fashion, in order to accurately measure small long-range couplings from the relative displacement between the two patterns in the other dimension (usually ω_2). Due to the possibility of isotope-selective excitation, the desired simplicity of the cross-peak patterns can be accom-

*Present address: Institut für Biophysikalische Chemie, Biozentrum, J.W. Goethe Universität, D-60439 Frankfurt am Main, Germany.
**To whom correspondence should be addressed.

plished without the phase-cycling procedures needed in homonuclear E.COSY experiments (Griesinger et al., 1985,1986,1987).

The design of special heteronuclear pulse experiments has provided more freedom in the optimization of measurement techniques for heteronuclear coupling constants. In particular, only strong one-bond and strong three-bond couplings can be exploited, both for the creation and for the E.COSY separation of the cross peaks. Techniques based on this principle have been proposed in the literature for the measurement of heteronuclear couplings (Sørensen, 1990; Eggenberger et al., 1992; Emerson and Montelione, 1992a,b; Seip et al., 1994; Weisemann et al., 1994a,b). The same procedure can also be used for the determination of homonuclear $^1H,^1H$ coupling constants in cases where the conventional homonuclear E.COSY spectra are not sufficiently resolved or the cross-peak intensity is too weak (Gemmecker and Fesik, 1991; Wagner et al., 1991; Emerson and Montelione, 1992a,b; Griesinger and Eggenberger, 1992; Madsen et al., 1993; Olsen et al., 1993a,b). Analogous techniques have been applied for the measurement of heteronuclear two-bond coupling constants (Delaglio et al., 1991; Vuister and Bax, 1992).

The measurement of heteronuclear J-coupling constants associated with a non-protonated carbon is particularly difficult. It is, for example, virtually impossible to determine these couplings from a homonuclear 2D spectrum. Of particular interest are the amino acid main-chain coupling constants $^3J_{H^N(i),C'(i)}$ and $^3J_{C'(i-1),H^\alpha(i)}$, and the side-chain coupling constants $^3J_{H^\beta(i),C'(i)}$ and $^3J_{H^\alpha(i),C'(i)}$ for a non-protonated γ carbon. In favourable cases, line shape deconvolution methods have been successfully applied to measure these couplings, since they appear as the active coupling in heteronuclear correlation peaks (Titman et al., 1989). Eggenberger et al. (1992) have described a SOFT-HCCH-COSY experiment which allows the measurement of $^3J_{H^\beta C'}$ from an E.COSY pattern generated by a two-step coherence transfer from $^{13}C^\alpha$ to H^β via $^{13}C^\beta$. This procedure has been expanded into a 3D experiment by Weisemann et al. (1994a) for $^{15}N,^{13}C$-labelled proteins. An analogous procedure can be applied for the measurement of $^3J_{H^N C'}$ (Seip et al., 1994; Weisemann et al., 1994b). These techniques are primarily based on efficient transfers through one-bond couplings.

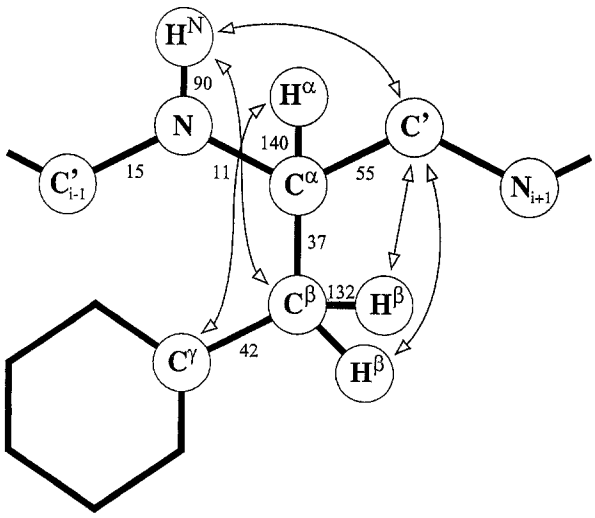

Fig. 1. Typical spin-coupling network encountered in polypeptides. The phenylalanine side chain is chosen as an example. The approximate magnitudes of the relevant one-bond J-coupling constants are indicated (in hertz). Arrows indicate the heteronuclear three-bond couplings examined in the present investigation.

In this paper we propose an alternative procedure for the measurement of heteronuclear three-bond couplings to non-protonated carbons by a heteronuclear relayed E.COSY technique which is characterized by a pulse sequence of great simplicity. To comply with the attempted simplicity, it is of advantage to use coherence transfers through the three-bond couplings $^3J_{H^\alpha H^N}$ or $^3J_{H^\alpha H^\beta}$. Despite the relative weakness of these couplings, it is shown by experiments on a uniformly ^{13}C-enriched sample of the antamanide that $J_{H^N C'}$, $J_{H^\beta C'}$, $J_{H^\alpha C'}$ and $J_{H^N C^\beta}$ (Fig. 1) can be measured with high accuracy from a single 2D data set. A convenient diagram is introduced to visualize the involved transfer and coupling pathways.

Methods

The concept

In the following, we designate the two active spins in an E.COSY-type experiment by A and B. They determine the position of the cross-peak multiplet at (Ω_A,Ω_B), which is separated in two patterns shifted by J_{AP} and J_{BP} along ω_1 and ω_2, respectively, by the passive spin P. It turns out that for the measurement of heteronuclear three-bond J-couplings to a non-protonated carbon, the potential couplings J_{AB} are too weak to produce a sufficiently strong cross peak. It is then necessary to transfer coherence in a relayed fashion (Eich et al., 1982), employing a relay spin R in the transfer sequence $A \rightarrow R \rightarrow B$.

The minimum spin system for the heteronuclear relayed E.COSY experiment is shown in Fig. 2a. A functional representation is depicted in Fig. 2b, where the two active spins are represented by the diagonal peaks of a virtual (ω_1,ω_2) 2D spectrum. The pathway of relayed coherence transfer is indicated by arrows, while the magnitude of the couplings to the passive spin P is visualized by heavy and light lines. The (A,B) cross peak is assumed to exhibit a large splitting in the ω_1 direction and a small one along ω_2. It is important to ensure that, during the relayed transfer, the spin state of the passive spin P is not changed. This scheme has been used before in homonuclear experiments for the measurement of long-range ^1H-^1H couplings (Schmidt et al., 1994) and in heteronuclear experiments (Montelione and Wagner, 1989; Sørensen, 1990; Eggenberger et al., 1992; Emerson and Montelione, 1992a,b; Seip et al., 1994; Weisemann et al., 1994a,b).

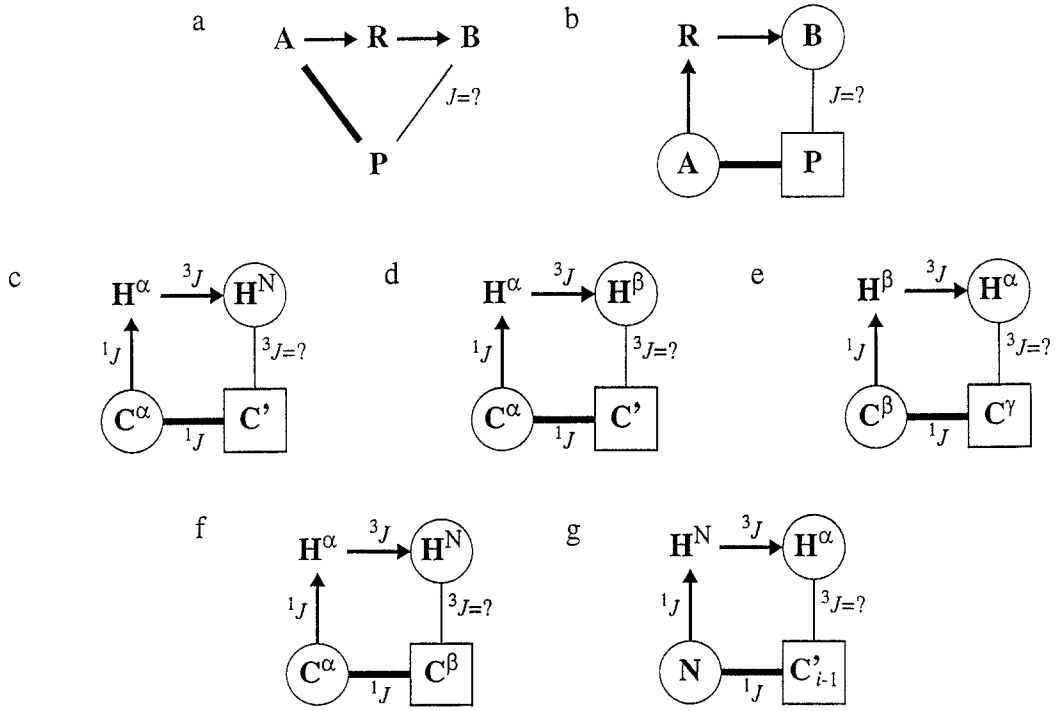

Fig. 2. Schematic representation of the spin-coupling networks used for the determination of multiple-bond coupling constants by heteronuclear relayed E.COSY. The basic four-spin subsystem (a) is redrawn in the form of a schematic 2D spectrum (b) with two encircled diagonal peaks A and B and a square cross peak with the desired E.COSY multiplet structure caused by spin P. Arrows indicate the active couplings which are essential for coherence transfer via the relay spin R. The passive spin P exhibits a strong coupling (thick line) used for separation of the two multiplet halves in ω_1, while the ω_2 separation represents the multiple-bond coupling to be measured (thin line). Schemes c, d, e and f are applicable to ^{13}C-enriched peptides, while scheme g requires ^{13}C,^{15}N doubly labeled samples.

The intent here is to design an experiment of maximum simplicity. For the optimum choice of the four spins A, B, P and R, let us consider the three typical situations indicated in Figs. 2c–e. In all of them, a J-coupling constant to a non-protonated carbon must be measured. It is mandatory to select this carbon as the passive spin P when proton polarization and/or proton observation should be used. The selection of the relay spin R is less obvious. It seems most appropriate to choose exclusively coherence transfers through strong one-bond couplings. For example, for the measurement of $^3J_{C'H^\beta}$ it would be possible to make the selection $A = C^\alpha$, $R = C^\beta$ and $B = H^\beta$, using $^1J_{C^\alpha C^\beta}$ and $^1J_{C^\beta H^\beta}$ for the relayed transfer and $^1J_{C'C^\beta}$ for the E.COSY dispersion, as employed by Eggenberger et al. (1992). It turns out that a much simpler pulse sequence results when $R = H^\alpha$ is chosen, as shown in Fig. 2d. The disadvantage that the relayed transfer involves the weaker $^3J_{H^\alpha H^\beta}$ coupling is offset by the possibility to use an efficient heteronuclear multiple-quantum coherence (HMQC) scheme. This is possible because the polarization used to polarize spin A stems from the relay spin R, such that a two-way heteronuclear transfer through the same pathway is possible. Similar arguments fixed the choice of the relay spin R in the schemes of Figs. 2c and e.

Minimum-length pulse sequence

Pulse sequences suitable for heteronuclear relayed E.COSY experiments are shown in Fig. 3. They apply to situations c–f in Fig. 2. Starting with H^α (or H^β) polarization, heteronuclear two-spin coherence is created by the sequence $(\pi/2)_{^1H}$-τ-$(\pi/2)_{^{13}C}$, where $\tau \sim (2\,^1J_{CH})^{-1}$. During t_1, the two-spin coherence senses the C^α (or C^β) chemical shift and the neighbor spin states mediated through the $^1J_{C^\alpha C'}$ and $^1J_{C^\alpha C^\beta}$ (or $^1J_{C^\beta C^\gamma}$ and $^1J_{C^\beta C^\alpha}$) couplings. At the same time, antiphase coherence is generated due to the coupling $^3J_{H^\alpha H^N}$ (or $^3J_{H^\alpha H^\beta}$). At the end of the t_1 period, proton single-quantum coherence is reestablished by a ^{13}C pulse that is selected, as described below, to have a small effect on the spin state of the passive spins C', C^β (or C^γ, C^α). After refocusing of the antiphase coherence due to the coupling $^1J_{CH}$ during the period τ, a relay mixing pulse $(\pi/2)_{^1H}$ is applied that transfers the coherence to the detection spin H^N, H^β, or H^α.

Three possibilities to prevent a mixing of the states of the passive spin P during the relayed coherence transfer are indicated in Figs. 3a–c: (i) application of frequency-selective ^{13}C pulses (Fig. 3a); (ii) application of small-flip-angle ^{13}C pulses (Fig. 3b); and (iii) application of E.COSY phase-cycling procedures (Fig. 3c).

For the present work, we have chosen the application of a ^{13}C pulse with a small flip angle, because this eliminates the need for phase cycling, and it is still applicable when frequency selectivity is difficult to achieve experimentally.

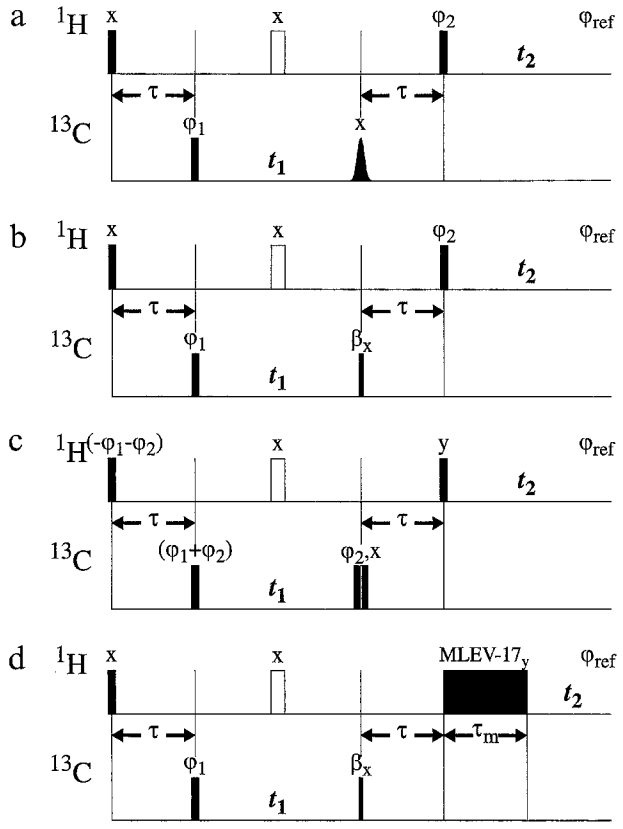

Fig. 3. Pulse sequences for the determination of heteronuclear three-bond couplings. Filled rectangular bars represent π/2 pulses (unless the flip angle β is indicated) and open bars represent π pulses. The complementary E.COSY spectrum is obtained with β_x replaced by $(\pi-\beta)_x$ in the small-flip-angle experiments (b) and (d); in the other approaches an additional π pulse on the ^{13}C channel may be used at the end of the refocussing period τ. (a) Heteronuclear relayed E.COSY sequence using a selective ^{13}C mixing pulse to prevent transitions of the passive nuclei. (b) Heteronuclear relayed E.COSY sequence using a nonselective small-flip-angle mixing pulse; $\beta_x = 35°$ is chosen to achieve reasonable suppression of unwanted multiplet components. The minimum phase cycle is φ_1 = x,–x,x,–x, φ_2 = y,y,–y,–y, φ_{ref} = x,–x,x,–x. In practice, supercycles are used that include inversion of the 180° refocussing pulse phase and of both ^{13}C pulse phases without altering the receiver phase. In addition, the phase of the excitation pulse can be inverted with concomitant inversion of the receiver phase. (c) Heteronuclear relayed E.COSY using phase cycles for spectral editing. The minimum phase cycle is φ_2 = 0°, 60°, 120°, 240°, 300°, φ_{ref} = 4×(0°), 3×(180°), 1×(0°), 1×(0°), 3×(180°); the multipliers indicate the amplitude weights. (d) Heteronuclear relayed E.COSY using a spin-lock sequence instead of a (π/2) proton pulse for mixing. This scheme leads to in-phase multiplets in the spectrum. The minimum phase cycle is φ_1 = x,–x, φ_{ref} = x,–x. If overlap is a problem, it is possible to utilize an additional ^{13}C-refocused multiple-quantum evolution period in a 3D ^{13}C,^{1}H,^{1}H-experiment by inserting a $t_3/2-(\pi)_C-t_3/2$ period immediately before or after the ^{1}H-refocussing pulse. Note that the additional carbon refocussing pulse would give rise to a complementary E.COSY pattern.

The basic pulse sequence is essentially a small-flip-angle relay variant of the HMQC-COSY sequence (Frey et al., 1985; Lerner and Bax, 1986; Clore et al., 1988; Gronenborn et al., 1989). It is also possible to replace the relay mixing pulse by a short TOCSY mixing period when in-phase multiplets are desired (Fig. 3d).

Response calculation

We concentrate on a heteronuclear four-spin system and identify in the following the two active spins A and B with S_1 and I_2, respectively, the relay spin R with I_1 and the passive spin P with S_2. We assume, as in Fig. 2, $J_{I_1S_2} = J_{I_2S_1} = 0$ and obtain the following expression for the density operator after the first two π/2 pulses, starting with $\sigma_0 = I_{1z}$:

$$\sigma(\tau,t_1=0) = -2S_{1y}[I_{1x}\cos(\pi J_{I_1I_2}\tau) + 2I_{1y}I_{2z}\sin(\pi J_{I_1I_2}\tau)] \quad (1)$$

provided that τ is adjusted to $(2J_{I_1S_1})^{-1}$ and φ_1 is set to the x phase. The I-spin chemical shift precession can be disregarded, because of the π refocusing pulse. The relevant spin operators containing S_{1y}, sensitive to the $(\beta_x)_S$ pulse at the end of the t_1 interval, are given by:

$$\begin{aligned}\sigma(\tau,t_1) = &-2S_{1y}[\cos(\pi J_{S_1S_2}t_1)\cos(\omega_{S_1}t_1)\\ &-2S_{2z}\sin(\pi J_{S_1S_2}t_1)\sin(\omega_{S_1}t_1)]\\ &\times[I_{1x}\cos(\pi J_{I_1I_2}(\tau+t_1))\\ &+2I_{1y}I_{2z}\sin(\pi J_{I_1I_2}(\tau+t_1))]\end{aligned} \quad (2)$$

For a weak $(\beta_x)_S$ pulse it is possible to neglect its influence on the spin S_2, and after the refocusing period τ, Eq. 3 is obtained:

$$\begin{aligned}\sigma(\tau,t_1,\tau) = &-\sin\beta[\cos(\pi J_{S_1S_2}t_1)\cos(\omega_{S_1}t_1)\\ &-2S_{2z}\sin(\pi J_{S_1S_2}t_1)\sin(\omega_{S_1}t_1)]\\ &\times[I_{1y}\cos(\pi J_{I_1I_2}(2\tau+t_1))\\ &-2I_{1x}I_{2z}\sin(\pi J_{I_1I_2}(2\tau+t_1))]\end{aligned} \quad (3)$$

The I_y term in the second bracket does not contribute to the observed cross peak and can be neglected. After the $(\pi/2)_y$ proton mixing pulse, we find for the coherence term responsible for the S_1I_2 cross peak:

$$\begin{aligned}\sigma(\tau,t_1,\tau,t_2=0) = &-2I_{1z}I_{2x}\sin\beta\sin(\pi J_{I_1I_2}(2\tau+t_1))\\ &\times[\cos(\pi J_{S_1S_2}t_1)\cos(\omega_{S_1}t_1)\\ &-2S_{2z}\sin(\pi J_{S_1S_2}t_1)\sin(\omega_{S_1}t_1)]\end{aligned} \quad (4)$$

In terms of the polarization operators $S_2^\alpha = 1/2 + S_{2z}$ and $S_2^\beta = 1/2 - S_{2z}$ and the frequencies

$$\Sigma_1 = \omega_{S_1} + \pi J_{S_1S_2} \quad (5a)$$

and

$$\Delta_1 = \omega_{S_1} - \pi J_{S_1S_2} \quad (5b)$$

one can recast Eq. 4 in the form

$$\begin{aligned}\sigma(\tau,t_1,\tau,t_2=0) = &-2I_{1z}I_{2x}\sin\beta\sin(\pi J_{I_1I_2}(2\tau+t_1))\\ &\times[S_2^\alpha\cos(\Sigma_1t_1) + S_2^\beta\cos(\Delta_1t_1)]\end{aligned} \quad (6)$$

The evolution during the detection period, finally, takes the form:

$$\begin{aligned}\sigma(\tau,t_1,\tau,t_2) = &-\sin\beta\sin(\pi J_{I_1I_2}(2\tau+t_1))\\ &\times\{S_2^{\alpha}\cos(\Sigma_1 t_1)[2I_{1z}I_{2x}\cos(\Sigma_2 t_2)\cos(\pi J_{I_1I_2}t_2)\\ &+I_{2y}\cos(\Sigma_2 t_2)\sin(\pi J_{I_1I_2}t_2)\\ &+2I_{1z}I_{2y}\sin(\Sigma_2 t_2)\cos(\pi J_{I_1I_2}t_2)\\ &-I_{2x}\sin(\Sigma_2 t_2)\sin(\pi J_{I_1I_2}t_2)]\\ &+S_2^{\beta}\cos(\Delta_1 t_1)[2I_{1z}I_{2x}\cos(\Delta_2 t_2)\cos(\pi J_{I_1I_2}t_2)\\ &+I_{2y}\cos(\Delta_2 t_2)\sin(\pi J_{I_1I_2}t_2)\\ &+2I_{1z}I_{2y}\sin(\Delta_2 t_2)\cos(\pi J_{I_1I_2}t_2)\\ &-I_{2x}\sin(\Delta_2 t_2)\sin(\pi J_{I_1I_2}t_2)]\}\end{aligned} \quad (7)$$

with

$$\Sigma_2 = \omega_{I_2} + \pi J_{I_2S_2} \quad (8a)$$

and

$$\Delta_2 = \omega_{I_2} - \pi J_{I_2S_2} \quad (8b)$$

The observable terms $S_2^m I_{2y}$ (and $S_2^m I_{2x}$ for quadrature detection), where $m=\alpha,\beta$, lead to two antiphase squares with the active coupling constant $2\pi J_{I_1I_2}$ at positions (Σ_1,Σ_2) and (Δ_1,Δ_2). This is the expected typical E.COSY pattern that allows the determination of the desired coupling constant $J_{I_2S_2}$ from the displacement

$$J_{I_2S_2} = \frac{\Sigma_2 - \Delta_2}{2\pi} \quad (9)$$

In practice, when the $(\beta_x)_S$ pulse is not sufficiently weak, a small perturbation by an additional complementary E.COSY contribution with a relative amplitude given by $\tan^2(\beta/2)$ must be expected. It can easily be taken into account in a quantitative computer analysis of the multiplet structure (Schmidt et al., 1994). Another potential reason for the appearance of a complementary E.COSY pattern is longitudinal relaxation between the t_1 and t_2 periods (Montelione et al., 1992). The limited length of this period in the experiments of Figs. 3a–c, $\tau \approx 3.5$ ms, minimizes these effects.

Determination of three-bond couplings in polypeptides

In the following, we will refer to the spin topologies typical of peptide chains (Fig. 1). It is assumed that the carbon sites are ^{13}C-labeled. For determining the backbone angle ϕ in an amino acid residue, six three-bond J-coupling constants can be used: $^3J_{HN^HH\alpha}$, $^3J_{HN^HC'}$, $^3J_{HN^HC\beta}$, $^3J_{C'(i-1),H\alpha(i)}$ $^3J_{C'(i-1),C\beta(i)}$ and $^3J_{C'(i-1),C'(i)}$. $^3J_{HN^HC'}$ and $^3J_{HN^HC\beta}$ will be determined in the context of the present investigation. A method is also proposed to determine the coupling constant $^3J_{C'(i-1),H\alpha(i)}$ in uniformly ^{13}C,^{15}N doubly enriched peptides. Assuming the presence of a $C^{\beta}H_2^{\beta}$ group, the side-chain dihedral angle χ_1 can be determined from a total of nine coupling constants, among them $^3J_{H\alpha H\beta 2}$, $^3J_{H\alpha H\beta 3}$, $^3J_{H\beta 2C'}$, $^3J_{H\beta 3C'}$, $^3J_{H\beta 2N'}$, $^3J_{H\beta 3N'}$ and $^3J_{H\alpha C\gamma}$. We discuss here the measurement of the $^3J_{HC}$ coupling constants. If ^{15}N-enriched material is available, analogous measurements apply to $^3J_{HN}$ couplings.

Determination of $^3J_{HN^HC'}$

For the determination of the coupling constant $^3J_{HN^HC'}$ by the pulse sequences of Fig. 3 and the scheme of Fig. 2c, a coherence transfer from C^{α} to H^N must be accomplished. The H^{α} proton acts as the relay spin, while C' is the passive spin. The one-bond coupling between C^{α} and C' of approximately 55 Hz is used for the separation of C^{α},H^N cross-peak components in ω_1. The small $^3J_{HN^HC'}$ coupling is then determined from the difference in the ω_2 coordinates. The $^2J_{HN^HC\alpha}$ coupling would provide a direct pathway for coherence transfer, but this coupling constant is usually too small (on the order of a few hertz) for an efficient transfer.

Determination of $^3J_{HN^HC\beta}$

As a bonus, the coupling constant $^3J_{HN^HC\beta}$ can be determined from the same cross peak as $^3J_{HN^HC'}$ discussed above. The passive spin C^{β} gives rise to an additional heteronuclear E.COSY-type pattern from which $^3J_{HN^HC\beta}$ can be determined according to the scheme of Fig. 2f. The passive one-bond coupling constant between the aliphatic C^{α} and C^{β} spins, used for the multiplet dispersion, is in the range 30–40 Hz. An alternative, perhaps even more straightforward, method for the determination of $^3J_{HN^HC\beta}$ has been demonstrated by Edison and co-workers (1991) using a homonuclear relayed COSY scheme.

Determination of $^3J_{H\beta C'}$

The heteronuclear three-bond coupling constant $J_{H\beta C'}$ can be determined from the (C^{α},H^{β}) cross peak in the heteronuclear relayed E.COSY spectrum, obtained also with the pulse sequences of Fig. 3, where again the coupling constant $^1J_{C\alpha C'}$ is exploited for separation following Fig. 2d. The direct coupling between the detected H^{β} proton and its attached carbon causes a large splitting in ω_2, which may lead to overlap problems when the chemical shifts of the two H^{β} protons are similar.

Determination of $^3J_{H\alpha C\gamma}$

For aromatic amino acid side chains, the coupling constant $^3J_{H\alpha C\gamma}$ can be retrieved, according to Fig. 2e, from the (C^{β},H^{α}) cross peak in the heteronuclear relayed E.COSY spectrum, again recorded with the pulse sequences of Fig. 3. The determination depends on the dispersion by the passive coupling of approximately 40 Hz between C^{β} and C^{γ}.

Determination of $^3J_{H^{\alpha}(i),C'(i-1)}$

The heteronuclear relayed E.COSY procedure can be applied to ^{15}N-labeled compounds for the determination of $^3J_{H\alpha(i),C'(i-1)}$, as indicated in Fig. 2g. The ^{15}N nucleus serves as the active spin, and the one-bond coupling $^1J_{C'(i-1),N(i)}$ functions as the E.COSY 'separator'. With a value of about 15 Hz, this coupling is relatively small. No selective or weak relay mixing pulse is necessary in this

case, as the passive ^{13}C spin is not affected by ^{15}N and ^{1}H pulses. Alternatively, $^{3}J_{C'(i-1),H^{\alpha}(i)}$ could be determined from the E.COSY-type splitting caused by the passive spin H^{α} in the (often weak) $C'(i-1)$-$C^{\alpha}(i)$ cross peak in a carbon COSY spectrum.

Experimental section

The heteronuclear relayed E.COSY experiment of Fig. 3b was applied for the measurement of three-bond J-coupling constants in the cyclic decapeptide antamanide, which is known to exhibit backbone dynamics resulting in an averaging of the J-coupling constants (Mádi et al., 1990; Brüschweiler et al., 1991; Ernst et al., 1991; Blackledge et al., 1993). To identify the involved conformations, as many geometric constraints as possible are required. The heteronuclear three-bond J-coupling constants measured in the present work form part of this data set.

Sample preparation

Uniformly ^{13}C-labeled antamanide was synthesized from commercially available ^{13}C-enriched amino acids. The linear peptide Pro-Ala-Phe-Phe-Pro-Pro-Phe-Phe-Val-Pro was prepared by standard solid-phase synthesis, starting from Boc-Pro-PAM-resin (Mitchell et al., 1978). The peptide (101 mg) was cyclized in the presence of *p*-nitrophenol (139 mg) and 1-(3-dimethylaminopropyl)-3-ethylcarbodiimide hydrochloride (155 mg) in a mixed solvent of 1-methyl-2-pyrrolidone (20 ml) and chloroform (20 ml). Antamanide (30 mg) was isolated from the reaction mixture by reversed-phase HPLC. The ^{13}C abundance was measured to be 98.6% by mass spectrometry. For the NMR measurements, antamanide was dissolved in deuterated chloroform at a concentration of approximately 20 mM.

Spectrum acquisition

The NMR experiment was performed on a Bruker AMX-500 spectrometer at 310 K using the pulse sequence of Fig. 3b. The delay τ for the evolution of ^{1}H-^{13}C one-bond couplings was set to 3.57 ms. By positioning the ^{13}C rf carrier frequency at the center of the aliphatic carbon resonances and adjusting the spectral width to 7576 Hz, the aromatic carbon resonances were folded onto the methyl carbon region of the spectrum, which were both of no direct interest. The TPPI method was used to distinguish positive and negative frequencies in the ω_1 dimension. The proton spectral width in ω_2 was 5556 Hz, with the audio filter frequency set to the same value to minimize aliased noise. The delay of the proton signal acquisition required a 180° linear phase correction after Fourier transformation, resulting in an optimally flat baseline (Marion and Bax, 1988). The acquisition times were 369 and 102 ms in the t_2 and t_1 dimensions, respectively. In the t_2 detection period, 4K data points were recorded. For each of the 1536 t_1 increments, 16 transients were accumulated with the phase cycle given in the caption of Fig. 3b. The spectrum was recorded within 12 h.

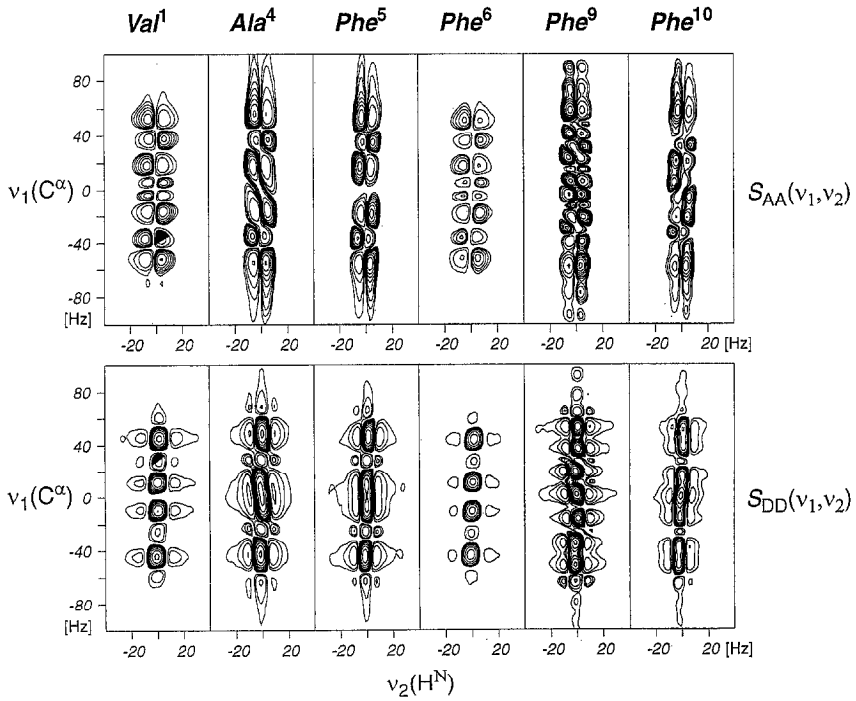

Fig. 4. Pure 2D absorptive S_{AA} and pure 2D dispersive S_{DD} parts of the experimental (C^{α},H^{N}) multiplets of ^{13}C-enriched antamanide, obtained with the heteronuclear relayed E.COSY pulse sequence depicted in Fig. 3b. Positive and negative contours are drawn with levels increasing by factors of $\sqrt{2}$ and 2, respectively.

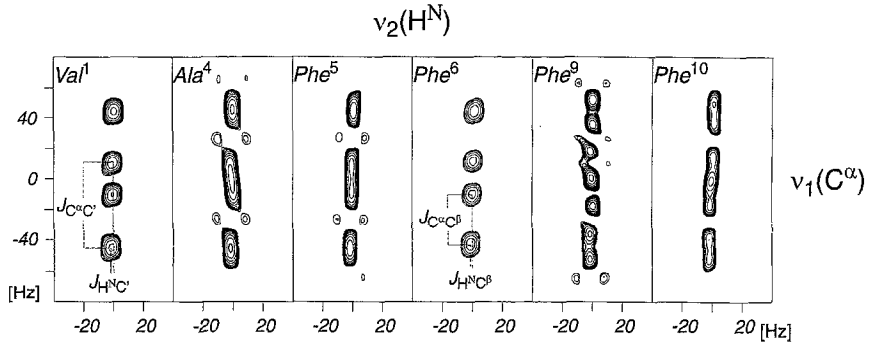

Fig. 5. Dispersive multiplets of the spectrum in Fig. 4, showing positive contour levels only. From these cross peaks, the heteronuclear coupling constants $^3J_{H^NC\beta}$ and $^3J_{H^NC'}$ were determined. At 310 K, the multiplets are located at the following (ν_1,ν_2) coordinates, given in ppm: Val[1] (56.4,7.57), Ala[4] (49.6,7.95), Phe[5] (56.7,6.96), Phe[6] (52.2,7.81), Phe[9] (57.3,7.35) and Phe[10] (58.9,7.24).

Spectrum processing

The data matrix was Fourier-transformed to 2K×2K hypercomplex points using zero-filling in the ω_1 dimension. The spectral resolutions were 3.699 and 2.713 Hz in the ω_1 and ω_2 dimensions, respectively. Prior to the Fourier transformation with respect to t_2, moderate resolution enhancement was applied by multiplication of the FID with a Gaussian function with a width $\delta = t_{1max}/4 =$ 93 ms and its maximum centered at $t_{2max}/5 = 74$ ms. A cosine window function was used for apodization in t_1. The first t_1 point was multiplied by 0.8 in order to achieve minimal ridges along ω_1 in the spectrum (Otting et al., 1986). For the determination of the J-coupling constants, the 2D spectrum was phase-adjusted to display a pure 2D dispersion spectrum $S_{DD}(\omega_1,\omega_2)$ (Pelczer et al., 1991), as shown in Fig. 4. However, the 2D mixed-phase spectrum $S_{DA}(\omega_1,\omega_2)$ was also retained to facilitate the evaluation of the multiplets.

J-coupling evaluation

The relative shift along the ω_2 direction between the two relevant E.COSY multiplet patterns yields the desired coupling constant. Representative projections were calculated from ω_2 sections taken through the two multiplet halves. In the simplest version, one of the two sections is then shifted pointwise to achieve an optimum superposition of the two sections. The accuracy of the J-coupling constant determined can be increased by application of zero-filling in the t_2 domain before resolution enhancement (Griesinger et al., 1987). Alternatively, the centers of gravity of the two multiplet halves may be computed from the 2D spectrum. The two passive coupling constants are then obtained from the coordinate differences in ω_1 and ω_2 (Montelione et al., 1992). For dissimilar patterns of the two multiplet halves, the results obtained by the two methods differ due to the presence of strong coupling, partial overlap, or differential relaxation effects (Görlach et al., 1993).

To avoid the limited accuracy of J-coupling determination by a sampling grid in the frequency space, we use here a least-squares fitting procedure in the t_2 time domain. The two sections $F(\omega_1^\alpha,\omega_2)$ and $F(\omega_1^\beta,\omega_2)$, taken from the two multiplet halves, are Fourier-transformed into the time domain to yield $f(\omega_1^\alpha,t_2)$ and $f(\omega_1^\beta,t_2)$, respectively. The indices α and β signify the spin states of the relevant passive spin.

A frequency shift of $F(\omega_1^\beta,\omega_2)$ by $2\pi J$ corresponds to a multiplication of $f(\omega_1^\beta,t_2)$ by the complex factor $\exp\{i2\pi Jt_2\}$. The least-squares fitting procedure has then the purpose of minimizing the expression

$$\varepsilon^2(J) = \sum_{k=0}^{n-1} \left| f(\omega_1^\alpha, k\Delta t_2) - \exp\{i2\pi Jk\Delta t_2\}\, f(\omega_1^\beta, k\Delta t_2) \right|^2 \quad (10)$$

as a function of J, where n is the number of sampling points with the time-domain separation Δt_2. The shift parameter J can assume arbitrary values and is not restricted to discrete values by a sampling grid.

Error calculation

The statistical error of the J value obtained can be computed by straightforward error propagation laws (Clifford, 1973). One obtains for the variance σ_J^2 of the J-coupling:

$$\sigma_J^2 = \sigma_f^2 \left\{ \sum_{k=0}^{n-1} \left| \frac{\partial}{\partial J} \left[f(\omega_1^\alpha, k\Delta t_2) - \exp\{i2\pi Jk\Delta t_2\}\, f(\omega_1^\beta, k\Delta t_2) \right] \right|^2 \right\}^{-1}_{J=J_{opt}} = \sigma_f^2 \left\{ \sum_{k=0}^{n-1} \left| 2\pi k\Delta t_2 \exp\{i2\pi J_{opt} k\Delta t_2\}\, f(\omega_1^\beta, k\Delta t_2) \right|^2 \right\}^{-1} \quad (11)$$

The variance σ_f^2 of the time-domain data can be estimated by the approximation

$$\sigma_f^2 \approx \frac{1}{n-1}\, \varepsilon^2(J_{opt}) \quad (12)$$

Results

The heteronuclear three-bond J-coupling constants in antamanide, determined by the heteronuclear relayed

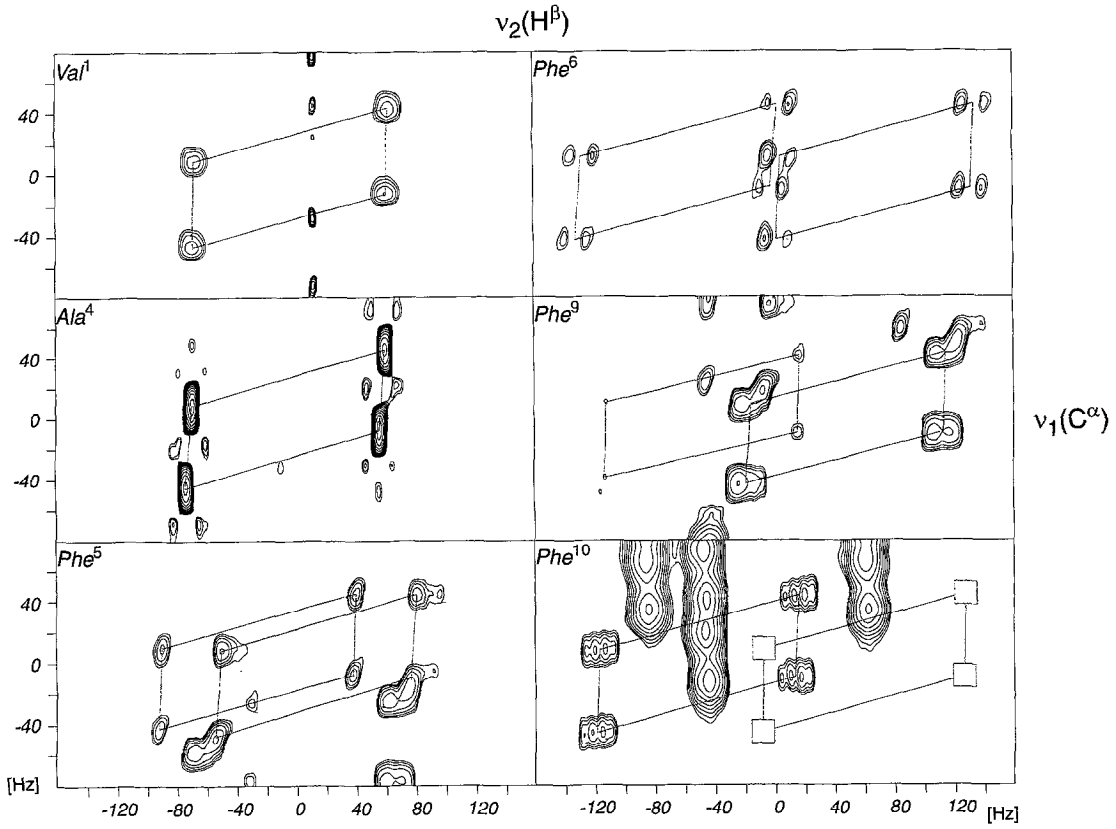

Fig. 6. Experimental (C^{α},$H^{\beta 2,3}$) multiplets from the dispersive heteronuclear relayed E.COSY spectrum of ^{13}C-enriched antamanide, showing positive contour levels only. From these cross peaks, the heteronuclear coupling constants $^3J_{H\beta 2C'}$ and $^3J_{H\beta 3C'}$ were determined. At 310 K, the multiplets are located at the following (ν_1,ν_2) coordinates, given in ppm: Val^1 (56.4,2.04), Ala^4 (49.6,1.10), Phe^5 (56.7,3.06/2.96), Phe^6 (52.2,3.18/2.91), Phe^9 (57.3,3.19/2.97) and Phe^{10} (58.9,3.38/3.15). The parallelograms indicate the relation of the constituent multiplet parts. The edges represent splittings along ν_1 and ν_2 due to the couplings $^1J_{C\alpha C'}$ and $^1J_{H\beta C\beta}$, respectively. The boxes indicate cross peaks below the plot level.

E.COSY experiment of Fig. 3, are listed in Table 1 for valine, alanine and phenylalanine residues. Since ^{13}C decoupling was avoided during acquisition, ^{13}C-bound protons gave rise to large splittings from heteronuclear one-bond couplings in the detection dimension (Figs. 6 and 7). As a consequence, a split relayed E.COSY pattern appears and the desired small passive couplings can be determined twice. The coupling constants in Table 1 are averaged values, i.e., $J = 1/2\,(J^- + J^+)$. The statistical error of the derived coupling constants is characterized by the standard deviation, conservatively calculated according to $\sigma_J = (\sigma_{J^-}^2 + \sigma_{J^+}^2)^{1/2}$.

$^3J_{HNC'}$ and $^3J_{HNC\beta}$ couplings

In the amide proton chemical-shift region of the heteronuclear relayed E.COSY spectrum, all six expected (C^{α},H^N) multiplets appear (Fig. 5). The H^N resonances of Val^1 and Phe^6 show appreciable line broadening, as has been reported before (Ernst et al., 1991). The $^3J_{HNC'}$ as well as the $^3J_{HNC\beta}$ coupling constants were found to be in the range 0–3 Hz.

$^3J_{H\beta C'}$ couplings

For each of the four phenylalanine residues, the heteronuclear coupling constants $^3J_{C'H\beta'}$ and $^3J_{C'H\beta''}$ were determined from the (C^{α},$H^{\beta'}$) and (C^{α},$H^{\beta''}$) cross peaks, respectively (Fig. 6). Values of up to 5.3 Hz were found. The unique $^3J_{C'H\beta}$ coupling constant in Val^1 was found to be 1.7 Hz. The $^3J_{C'H\beta}$ coupling constant in Ala^4 is conformationally averaged, due to rotation of the methyl group. A value of 4.0 Hz was found.

$^3J_{H\alpha C\gamma}$ couplings

The $^3J_{H\alpha C\gamma}$ coupling constants in phenylalanine residues were determined from the (C^{β},H^{α}) cross peak (Fig. 7). The similar one-bond couplings $^3J_{C\beta C\gamma'}$ and $^3J_{C\beta C\gamma''}$ in Val^1 cause overlap of the central multiplet components in ω_1. Therefore, only the sum of the two $^3J_{H\alpha C\gamma}$ coupling constants could be determined from the outer multiplet components. With the aid of ^{13}C-ω_1-filtered TOCSY experiments, it was possible to determine also their difference, leading to values of 2.8 and 3.3 Hz for the coupling constants $^3J_{H\alpha C\gamma'}$ and $^3J_{H\alpha C\gamma''}$, respectively.

Discussion

Based on known relations between dihedral bond angles and three-bond J-coupling constants, it is possible

TABLE 1
EXPERIMENTAL THREE-BOND J(H,C) COUPLING CONSTANTS (Hz) ASSOCIATED WITH BACKBONE ϕ ANGLES OR SIDE-CHAIN χ_1 ANGLES IN ANTAMANIDE[a]

Residue	$^3J_{HNC'}$	$^3J_{H\beta'C'}$	$^3J_{H\beta''C'}$	$^3J_{H\alpha C\gamma}$	$^3J_{HNC\beta}$
Val[1]	1.12±0.18	1.74±0.43		6.15±1.43[b]	1.32±0.24
Ala[4]	0.14±0.07	3.96±0.13		–	1.79±0.08
Phe[5]	1.45±0.09	0.26±0.75	5.31±0.81	2.49±0.68	1.53±0.13
Phe[6]	1.82±0.31	5.33±0.42	2.10±0.37	4.55±0.36	1.10±0.28
Phe[9]	0.61±0.21	1.10±0.66	3.36±0.65	2.05±0.31	3.13±0.33
Phe[10]	2.73±0.20	3.57±0.12	0.22±0.25	2.53±0.61	0.81±0.22

[a] The coupling constants have been determined from a single heteronuclear relayed E.COSY spectrum. Prime and double prime designate low-field and high-field H^β resonances, respectively, irrespective of the stereospecific assignments.
[b] Only the sum of the two valine couplings $^3J_{H\alpha C\gamma 1}$ and $^3J_{H\alpha C\gamma 2}$ could be determined from the heteronuclear relayed E.COSY multiplet.

to deduce structural information from J-coupling measurements. We used for $^3J_{HNH\alpha}$, $^3J_{HNC'}$, $^3J_{HNC\beta}$ and $^3J_{H\alpha H\beta}$ the parameters by Bystrov (1976), for $^3J_{H\alpha C\gamma}$ the parameters by Wasylishen and Schaefer (1972), and for $^3J_{H\beta C'}$ the relation published by Fishman et al. (1979).

Coupling constants related to backbone dihedral angles

The $^3J_{HNC'}$ and $^3J_{HNC\beta}$ coupling constants measured for antamanide in chloroform solution supplement the homonuclear $^3J_{HNH\alpha}$ coupling constants determined previously (Griesinger et al., 1987; Kessler et al., 1989a) and provide additional dihedral angle constraints for the backbone angles ϕ. The $^3J_{HNC\beta}$ coupling constants are in agreement with values obtained from ^{13}C-ω_1-filtered TOCSY spectra recorded for natural abundance and ^{13}C-enriched samples (Schmidt, J.M., unpublished results). The determination of a unique backbone conformation based on the J-coupling data summarized in Table 1 failed, as found previ-

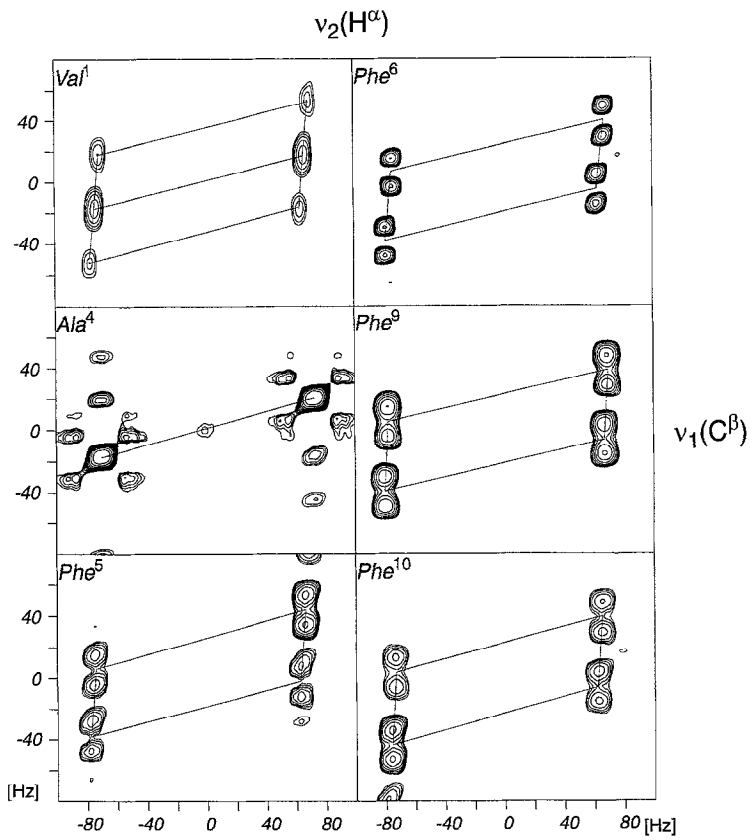

Fig. 7. Experimental (C^β,H^α) multiplets from the pure 2D dispersive heteronuclear relayed E.COSY spectrum of ^{13}C-enriched antamanide, showing positive contour levels only. From these cross peaks, the heteronuclear coupling constants $^3J(H^\alpha,C^\gamma)$ were determined. Note that the upper right multiplet part of Phe[5] coincides with the lower left part of the Phe[10] multiplet due to overlap. This overlap could be avoided by recording a complementary E.COSY spectrum with the flip angle β_x set to $(\pi-\beta)_x$. As the couplings $^1J_{C\beta C\gamma 1}$ and $^1J_{C\beta C\gamma 2}$ in Val[1] are similar, $^3J_{H\alpha C\gamma 1}$ and $^3J_{H\alpha C\gamma 2}$ coupling constants are difficult to be distinguished. At 310 K, the multiplets are located at the following (ν_1,ν_2) coordinates, given in ppm: Val[1] (31.1,4.46), Ala[4] (16.3,4.30), Phe[5] (35.7,4.07), Phe[6] (36.3,4.63), Phe[9] (37.9,4.57) and Phe[10] (35.1,3.78). The parallelograms indicate the relation of the constituent multiplet parts. The edges represent splittings along ν_1 and ν_2 due to the couplings $^1J_{C\beta C\gamma}$ and $^1J_{H\alpha C\alpha}$, respectively.

ously by using NOE data (Kessler et al., 1988,1989b; Ernst et al., 1991). The experimental J-coupling constants are interpreted as dynamically averaged data, and they were used to supplement NOE distance information in a conformational study (Blackledge et al., 1993).

Coupling constants related to side-chain rotameric states in phenylalanines

The analysis of the rotamer populations with respect to the χ_1 dihedral angle requires stereospecific assignments of phenylalanine $H^{\beta 2}$ and $H^{\beta 3}$ resonances, which have been obtained previously for Phe[9] and Phe[10] only (Kessler et al., 1987). For Phe[10], low-field and high-field H^{β} resonances have been assigned to $H^{\beta 2}$ and $H^{\beta 3}$, respectively, while for Phe[9] the assignment is opposite. Both side chains predominantly reside in a staggered rotamer state with $\chi_1 \approx -60°$, as has been concluded from the large difference in the homonuclear coupling constants $^3J_{H\alpha H\beta 2}$ and $^3J_{H\alpha H\beta 3}$ (Griesinger et al., 1987). The relative magnitudes of the $^3J_{H\beta 2C'}$ and $^3J_{H\beta 3C'}$ coupling constants, determined from heteronuclear relayed E.COSY spectra (Table 1), further consolidate the analysis by Kessler and coworkers (1987). The $^3J_{H\alpha C\gamma}$ coupling constants (Table 1) are in agreement with the proposed conformations.

For Phe[5] and Phe[6], the analysis of the side-chain rotamers is not as straightforward as for Phe[9] and Phe[10]. From the pair of similar (averaged) homonuclear $^3J_{H\alpha H\beta}$ coupling constants, it is inferred that a conformational equilibrium between at least two χ_1 states has to be considered. To obtain the proper dihedral angle distribution profiles, the H^{β} resonances must be unambiguously assigned to the respective diastereotopic proton positions. However, the two possible assignments cannot be distinguished unless recourse is taken to diastereospecific deuteration experiments. Based on the large dispersion in the heteronuclear coupling constants determined in this work, models are precluded that describe the side-chain conformational equilibria in Phe[5] and Phe[6] in terms of full rotational averaging.

Coupling constants in valine

As the methyl proton resonances are degenerate under the experimental conditions used here, the stereospecific assignment of the methyl carbons $C^{\gamma 1}$ and $C^{\gamma 2}$ cannot be deduced on the basis of J_{HC} coupling constants without knowledge of the side-chain conformation. The conformational analysis of the J-coupling constants turned out to be insensitive to the $C^{\gamma 1}$ and $C^{\gamma 2}$ resonance assignments. This is a consequence of the similarity of the two $J_{H\alpha C\gamma}$ coupling constants. From heteronuclear relayed E.COSY spectra, a small $J_{C'H\beta}$ coupling constant of approximately 1.7 Hz was found, while a large $^3J_{H\alpha H\beta}$ coupling constant of 13.8 Hz has been determined from homonuclear E.COSY multiplets at high (320 K) and low (256 K) temperature (Schmidt, J.M., unpublished results). These data indicate that the Val[1] side chain prefers a conformation with $\chi_1 \approx 180°$. This contrasts with X-ray results (Karle et al., 1979), which infer a small $^3J_{H\alpha H\beta}$ coupling constant of approximately 3–4 Hz due to a *gauche* orientation of the involved nuclei ($\chi_1 = -54.5°$). The NMR results agree with database statistics (Janin et al., 1978; Ponder and Richards, 1987) which assign an occurrence of 67% to the $\chi_1 \approx 180°$ state for valine side chains in proteins. Very recently, a detailed analysis of valine three-bond J-coupling constants in a protein has been published (Karimi-Nejad et al., 1994).

Conclusions

An essential feature of the heteronuclear relayed E.COSY pulse sequences proposed here is the intermediate creation of heteronuclear multiple-quantum coherence (HMQC) during the t_1 period. It is well known that sequences of this type lead to an efficient coherence transfer, as during t_1 proton–proton couplings and carbon chemical shifts evolve simultaneously. As a possible drawback, additional multiplet splittings appear in the ω_1 dimension due to proton–proton interactions. The creation of ^{13}C (antiphase) single-quantum coherence during t_1 (Bodenhausen and Ruben, 1980) would avoid the undesired splittings in the ω_1 dimension. However, the spectra could suffer from phase-modulated ω_1 multiplets due to evolution of the weak direct heteronuclear coupling $J_{S_1I_2}$ associated with the detected spin (B in Fig. 2). This effect arises during the second INEPT period τ used in such HSQC-type sequences. HMQC-type experiments are devoid of this problem. In view of applications to larger molecules like proteins, it is known that HMQC-type experiments may be superior to experiments involving heteronuclear single-quantum antiphase coherence due to slower relaxation (Seip et al., 1992).

The fact that the proposed heteronuclear relayed E.COSY experiment requires a minimum number of pulses renders it suitable for quantitative evaluation of the cross-peak multiplets by computer simulation and least-squares fitting to obtain accurate J-coupling constants. We support the view that a simple experiment, even if it might lead to somewhat lower sensitivity due to a transfer through a three-bond J coupling and the use of small-flip-angle pulses, can yield multiplet structures that are less prone to artefacts than more sophisticated pulse sequences using a multitude of selective and nonselective pulses.

Acknowledgements

This work was supported in part by a postdoctoral grant of the Deutsche Forschungsgemeinschaft to J.M.S. (Schm 854/1-1) and by the Swiss National Science Foundation. Measurement time on an AMX-500 spectrometer was kindly provided by Spectrospin AG, Fällanden, Switzerland.

References

Blackledge, M.J., Brüschweiler, R., Griesinger, C., Schmidt, J.M., Xu, P. and Ernst, R.R. (1993) *Biochemistry*, **32**, 10960–10974.

Bodenhausen, G. and Ruben, D.J. (1980) *Chem. Phys. Lett.*, **69**, 185–189.

Brüschweiler, R., Blackledge, M. and Ernst, R.R. (1991) *J. Biomol. NMR*, **1**, 3–11.

Bystrov, V.F. (1976) *Prog. NMR Spectrosc.*, **10**, 41–81.

Clifford, A.A. (1973) *Multivariate Error Analysis*, Applied Science Publishers Ltd., London.

Clore, G.M., Bax, A., Wingfield, P.T. and Gronenborn, A. (1988) *FEBS Lett.*, **238**, 17–21.

Delaglio, F., Torchia, D.A. and Bax, A. (1991) *J. Biomol. NMR*, **1**, 439–446.

Edison, A.S., Westler, W.M. and Markley, J.L. (1991) *J. Magn. Reson.*, **92**, 434–438.

Eggenberger, U., Karimi-Nejad, Y., Thüring, H., Rüterjans, H. and Griesinger, C. (1992) *J. Biomol. NMR*, **2**, 583–590.

Eich, G.W., Bodenhausen, G. and Ernst, R.R. (1982) *J. Am. Chem. Soc.*, **104**, 3731–3732.

Emerson, S.D. and Montelione, G.T. (1992a) *J. Am. Chem. Soc.*, **114**, 354–356.

Emerson, S.D. and Montelione, G.T. (1992b) *J. Magn. Reson.*, **99**, 413–420.

Ernst, R.R., Blackledge, M., Boentges, S., Briand, J., Brüschweiler, R., Ernst, M., Griesinger, C., Mádi, Z.L., Schulte-Herbrüggen, T. and Sørensen, O.W. (1991) In *Proteins: Structure, Dynamics and Design* (Eds, Renugopalakrishnan, V., Carey, P.R., Smith, I.C.P., Huang, S.G. and Storer, A.C.) ESCOM, Leiden, pp. 11–28.

Fishman, A.J., Live, D.H., Wyssbrod, H.R., Agosta, W.C. and Cowburn, D. (1979) *J. Am. Chem. Soc.*, **102**, 2533–2539.

Frey, M.H., Wagner, G., Vasak, M., Sørensen, O.W., Neuhaus, D., Wörgötter, E., Kägi, J.H.R., Ernst, R.R. and Wüthrich, K. (1985) *J. Am. Chem. Soc.*, **107**, 6847–6851.

Gemmecker, G. and Fesik, W. (1991) *J. Magn. Reson.*, **95**, 208–213.

Görlach, M., Wittekind, M., Farmer II, B.T., Kay, L.E. and Mueller, L. (1993) *J. Magn. Reson. Ser. B*, **101**, 194–197.

Griesinger, C., Sørensen, O.W. and Ernst, R.R. (1985) *J. Am. Chem. Soc.*, **107**, 6394–6396.

Griesinger, C., Sørensen, O.W. and Ernst, R.R. (1986) *J. Chem. Phys.*, **85**, 6837–6852.

Griesinger, C., Sørensen, O.W. and Ernst, R.R. (1987) *J. Magn. Reson.*, **75**, 474–492.

Griesinger, C. and Eggenberger, U. (1992) *J. Magn. Reson.*, **97**, 426–434.

Gronenborn, A., Bax, A., Wingfield, P.T. and Clore, G.M. (1989) *FEBS Lett.*, **243**, 93–98.

Janin, J., Wodak, S., Levitt, M.H. and Maigret, B. (1978) *J. Mol. Biol.*, **125**, 357–386.

Karimi-Nejad, Y., Schmidt, J.M., Rüterjans, H., Schwalbe, H. and Griesinger, C. (1994) *Biochemistry*, **33**, 5481–5492.

Karle, I.L., Wieland, T., Schermer, D. and Ottenheym, H.C.J. (1979) *Proc. Natl. Acad. Sci. USA*, **76**, 1532–1536.

Karplus, M. (1959) *J. Chem. Phys.*, **30**, 11–15.

Karplus, M. (1963) *J. Am. Chem. Soc.*, **85**, 2870–2871.

Kessler, H., Griesinger, C. and Wagner, K. (1987) *J. Am. Chem. Soc.*, **109**, 6927–6933.

Kessler, H., Griesinger, C., Lautz, J., Müller, A., Van Gunsteren, W.F. and Berendsen, H.J.C. (1988) *J. Am. Chem. Soc.*, **110**, 3393–3396.

Kessler, H., Müller, A. and Pook, K.-H. (1989a) *Liebigs Ann. Chem.*, 903–912.

Kessler, H., Bats, J.W., Lautz, J. and Müller, A. (1989b) *Liebigs Ann. Chem.*, 913–928.

Lerner, L. and Bax, A. (1986) *J. Magn. Reson.*, **69**, 375–380.

Mádi, Z.L., Griesinger, C. and Ernst, R.R. (1990) *J. Am. Chem. Soc.*, **112**, 2908–2914.

Madsen, J.C., Sørensen, O.W., Sørensen, P. and Poulsen, F.M. (1993) *J. Biomol. NMR*, **3**, 239–244.

Marion, D. and Bax, A. (1988) *J. Magn. Reson.*, **79**, 352–356.

Mitchell, A.R., Kent, S.B.H., Engelhard, M. and Merrifield, R.B. (1978) *J. Org. Chem.*, **43**, 2845–2852.

Montelione, G.T. and Wagner, G. (1989) *J. Am. Chem. Soc.*, **111**, 5474–5475.

Montelione, G.T., Winkler, M.E., Rauenbühler, P. and Wagner, G. (1989) *J. Magn. Reson.*, **82**, 198–204.

Montelione, G.T., Emerson, S.D. and Lyons, B.A. (1992) *Biopolymers*, **32**, 327–334.

Olsen, H.B., Ludvigsen, S. and Sørensen, O.W. (1993a) *J. Magn. Reson. Ser. A*, **104**, 226–230.

Olsen, H.B., Ludvigsen, S. and Sørensen, O.W. (1993b) *J. Magn. Reson. Ser. A*, **105**, 321–322.

Otting, G., Widmer, H., Wagner, G. and Wüthrich, K. (1986) *J. Magn. Reson.*, **66**, 187–193.

Pelczer, I., Bishop, K.D., Levy, G.C. and Borer, P.N. (1991) *J. Magn. Reson.*, **91**, 604–606.

Ponder, J.W. and Richards, F.M. (1987) *J. Mol. Biol.*, **193**, 775–791.

Schmidt, J.M., Sørensen, O.W. and Ernst, R.R. (1994) *J. Magn. Reson. Ser. A*, **109**, 80–89.

Schmieder, P., Kurz, M. and Kessler, H. (1991) *J. Biomol. NMR*, **1**, 403–420.

Seip, S., Balbach, J. and Kessler, H. (1992) *J. Magn. Reson.*, **100**, 406–410.

Seip, S., Balbach, J. and Kessler, H. (1994) *J. Magn. Reson. Ser. B*, **104**, 172–179.

Sørensen, O.W. (1990) *J. Magn. Reson.*, **90**, 433–438.

Titman, J.J., Neuhaus, D. and Keeler, J. (1989) *J. Magn. Reson.*, **85**, 111–131.

Vuister, G.W. and Bax, A. (1992) *J. Biomol. NMR*, **2**, 401–405.

Wagner, G., Schmieder, P. and Thanabal, V. (1991) *J. Magn. Reson.*, **93**, 436–440.

Wasylishen, R. and Schaefer, T. (1972) *Can. J. Chem.*, **50**, 2710–2712.

Weisemann, R., Löhr, F. and Rüterjans, H. (1994a) *J. Biomol. NMR*, **4**, 587–593.

Weisemann, R., Rüterjans, H., Schwalbe, H., Schleucher, J., Bermel, W. and Griesinger, C. (1994b) *J. Biomol. NMR*, **4**, 231–240.

Wider, G., Neri, D., Otting, G. and Wüthrich, K. (1989) *J. Magn. Reson.*, **85**, 426–431.

Wüthrich, K. (1986) *NMR of Proteins and Nucleic Acids*, Wiley, New York, NY.